Large-Scale Thermal Bending Fracture of Sea Ice Plates

Zdeněk P. Bažant

Department of Civil Engineering, Northwestern University, Evanston, Illinois

A hypothesis that large-scale fracture of sea ice plates in the Arctic could be caused by the release of energy of thermal bending moments due to major temperature changes is advanced and examined. Bending propagation of a through-the-thickness crack along the floating plate, with negligible inertial forces, is analyzed, assuming the moment field in the plate near the traveling crack front and the fracture process zone to be in a steady state. The analysis uses the plate-bending theory, and the second-order geometric effects of the in-plane normal forces are taken into account. Quasi-elastic behavior is assumed, and creep is treated approximately according to the effective modulus method. The calculated temperature difference between the top and bottom of the plate required to produce this kind of fracture is found to be well within the range that actually occurs in the Arctic, but this cannot be regarded as a proof of the hypothesis because of the simplifying assumptions made as well as uncertainties about large-scale fracture properties of sea ice. Further, it is shown that this type of fracture must exhibit a size effect, such that the critical temperature difference decreases in proportion to (plate thickness)$^{-3/8}$. This might explain why large fractures often form in an intact thick plate rather than only in a thin plate and along lines of weakness. For the case that the in-plane forces are significant, it is shown that beyond a certain critical crack length the thermally driven bending fracture (if it exists) must transit to a planar (nonflexural) fracture driven by the release of the energy of the in-plane forces generated by wind and ocean currents. The effect of creep is to increase the required critical temperature difference, as well as the critical crack length for the aforementioned transition. For thermal bending fracture, the minimum possible spacing of parallel cracks increases with the plate thickness and is independent of the crack length, while after transition to planar fracture it increases in proportion to the crack length. The hypothesis of thermal bending fracture cannot be proven or disproven without new types of experiments and measurements in the Arctic, and their computer modeling.

1. Introduction

Observations of the ice in the Arctic Ocean indicate that long fractures many miles in length form almost instantaneously. Rather than following the existing lines of weakness such as thin refrozen leads between the floes, these new fractures typically cut through intact pack ice floes, as well as through old and new pressure ridges [*Assur*, 1963]. They may serve as the initial triggering events for the opening of leads as well as the formation of new pressure ridges or rafting.

Large-scale tensile fractures can of course be produced by forces induced in the ice plate by wind and ocean currents. There are, however, two observations which suggest that another mechanism might also be at work, especially at the beginning of fracture propagation: (1) The forces in the ice plates are usually compressive, not tensile. Although fracture is still possible under compression, in the form of either axial splitting cracks or compression crushing, the former seems to require very large forces, and the latter would be unlikely to occur in intact thick ice plates. (2) If tensile fracture were the only mechanism, the fractures would have to form mainly along the lines of weakness, such as the thin ice in thin refrozen leads, and not through intact thick ice plates (the fact that young, thin ice, owing to its higher

salinity, is more ductile does not mitigate this argument because even plastic deformation of such thin ice would have to occur first, thereby relieving the forces).

Another possible mechanism is of thermal origin. Expanding on a previous brief conference presentation [*Bažant*, 1992], this paper will explore this idea from the fracture mechanics viewpoint and advance the hypothesis that thermal bending moments in the ice plate might play a significant role as the driving force of such fractures. Attention will be focused mainly on the size effect, in order to deduce whether or not such fractures would be more likely to occur in thinner plates. Although a better, more detailed solution could be carried out numerically by the finite element method, better insight and understanding of the problem can be gained by an analytical solution, even if simplifications are introduced. Thus the objective of this paper is an analytical solution capturing, hopefully, the main trends. Considerable simplifications will be required to make such a solution feasible.

2. Current Status and Problems of Fracture Mechanics of Ice

It has been well known that thermal stresses in sea ice plates are large enough to cause cracking [e.g., *Sanderson*, 1988]. Acoustic emissions from thermal fracturing events have been recorded [e.g., *Milne*, 1972; *Farmer and Xie*, 1989; *Lewis and Denner*, 1988]. Thermal cracking of sea ice plates has been studied by *Evans and Untersteiner* [1971] and *Evans* [1971], but on the basis of the strength theory

rather than fracture mechanics. However, as is now well understood, the strength theory can govern only crack initiation, not propagation. Growth of thermal cracks through the thickness of ice plates was analyzed by *Gold* [1971], and the stress singularities associated with such growth have been studied by *Parmerter* [1975]. But our interest here is in large-scale propagation of through cracks along the ice plate, over distances at least 10 m and typically many miles.

Thermal stresses have in the past been dismissed as a possible cause of large fractures, but this is not necessarily correct. It has been argued that from heat conduction calculations [e.g., *Sanderson*, 1988], the temperature fluctuations of the environment can penetrate only a small portion of the thickness of a thick ice plate. This apparently suggests that the thermal cracks could not become long enough to spread across the whole thickness of the plate. But this argument is fallacious.

The fallacy of this argument is that it tacitly limits attention only to cracks that form without any bending of the plate. It neglects the possibility that even thermal stresses confined to a thin layer near the top surface may suffice to cause a significant bending moment. As we will see, the release of the strain energy of the bending moment field in the plate can be large enough to produce thermal cracks through the whole thickness.

Now it is important to note that major fractures could conceivably form in this manner regardless of whether the plate is in tension or compression. Because the thicker an undamaged ice plate, the greater is the thermal bending moment, it might be possible to explain why thick intact plates are apparently not less likely to fracture than thin plates or plates damaged by prior fracturing.

Fracture mechanics of ice has been studied extensively and much has already been learned [e.g., *Anderson*, 1960; *Sanderson*, 1988; *Urabe and Yoshitake*, 1981; *Bentley et al.*, 1988; *DeFranco and Dempsey*, 1990, 1991; *Dempsey 1989, 1990*; *Dempsey et al.*, 1989a, b, 1990, 1991; *Ketcham and Hobbs*, 1969; *Palmer et al.*, 1983; *Parsons*, 1991; *Parsons et al.*, 1987, 1988, 1989; *Stehn*, 1990; *Timco*, 1991; *Timco and Sinha*, 1988; *Weeks and Mellor*, 1984; and references therein]. Reviewing the existing knowledge is beyond the scope of this work.

It appears, however, that most of the existing studies have been confined predominantly to the laboratory scale. No fracture test data appear to exist for large-scale fracture of ice plates, with all their inhomogeneities, such as the brine pockets, prior microcracks or larger fissures, and large ice blocks delineated by surfaces of weakness (e.g., refrozen cracks). Obtaining such data would require tests of large floating fracture specimens cut from the sea ice plate in the Arctic. In the meantime, one must rely on theoretical deductions, drawing from analogy with other materials of similar fracture behavior, for example, concrete, modern toughened ceramics, or some rocks. The basic properties that ice has in common with these so-called quasi-brittle materials are (1) low tensile strength, (2) large size inhomogeneities with weak interfaces, and large pores, (3) residual stresses, and (4) prior damage (microcracking and cracking). For these materials it is known that the fracture process zone surrounding the tip of a major crack is 1 to 2 orders of magnitude larger than the largest inhomogeneities. The same is likely to be true of ice.

For example, the process zone size in hardened cement paste is only a fraction of a millimeter. But in dam concrete, in which the largest aggregate pieces may be 0.25 m in size, the effective process zone size may be many meters. A similar picture must be expected for sea ice. For pure ice, material scientists have determined that the process zone size is less than a centimeter, but assuming the same to hold for through-the-thickness cracks in sea ice plates would be totally unreasonable.

The existence of such a large fracture process zone can be confirmed, in mechanics terms, by the size effect method [*RILEM Committee TC89-FMT*, 1990], on the basis of measured deviations from the size effect of linear elastic fracture mechanics (LEFM). Such tests may eventually have to be carried out in the Arctic. The fracture energy, that is, the energy dissipated by the fracture process zone per unit advance of a major crack, could certainly be much larger than the fracture energy of a crack in pure ice because the dissipated energy increases in proportion to the size of the process zone, but it could also be about equal because this increase may be offset by the fact that in a thick inhomogeneous plate the cracking may occur preferentially at weaker interfaces.

An important aspect of fracture phenomena is the size (or scale) effect, which will represent the focus of our analysis. The size effect has currently emerged as a topic of major interest for ocean ice dynamics [*Curtin*, 1991]. The size effect is understood as the dependence of the nominal strength (nominal stress at maximum load) on the structure size, provided that geometrically similar situations are compared. In linear elastic fracture mechanics of two- and three-dimensional bodies, the nominal strength is proportional to $(\text{size})^{-1/2}$, which is the strongest deterministic size effect possible. When the material failure condition is expressed in terms of stresses and strains, there is no size effect. This is for example the case for plastic limit analysis and for elastic (nonfracture) analysis with strength (or allowable stress) limit. In the case of thermal fracture, the nominal stress is proportional to the temperature difference, and so the size effect is characterized by the size dependence of the critical temperature difference required to cause fracture propagation. For quasi-brittle materials, the size effect may be described by an approximate law proposed by *Bažant* [1984], which represents a gradual transition between the size effects of the strength theory and of LEFM, the former being asymptotically approached for sufficiently small structures and the latter for sufficiently large structures.

The size effect in the strength of structures, including ice, has traditionally been explained by the randomness of material strength, as described by Weibull's statistical theory [e.g., *Butiagin*, 1966]. Recently, however, it has been shown that this explanation is incorrect for quasi-brittle materials in which large crack growth can occur prior to failure [*Bažant and Xi*, 1990]. The energy release and stress redistributions caused by large crack growth cause a strong deterministic size effect. This is due to the fact that a larger structure stores more strain energy. Thus if the nominal stress at failure were the same, more energy would be released into the fracture front. But the energy dissipated by at the fracture front (i.e., the fracture energy) is the same regardless of structure size. So the nominal stress at failure of a larger structure must be smaller. For structures with large cracks, this deterministic effect makes the statistical

effect secondary and unimportant. The Weibull-type statistical size effect dominates only if failure occurs while the crack is still very small, microscopic, which is normally true for metallic structures but almost certainly not for sea ice plates. It may be noted that *Bažant and Kim* [1985] have already shown that the aforementioned deterministic size effect does not disagree with Butiagin's test data for lake ice.

3. Bending Energy Release and Dissipation

Consider an infinitely extending ice plate of thickness h floating on water of specific weight ϱ (Figure 1a). For the sake of simplicity, we first assume the plate to be elastic but we will take creep approximately into account later. Let x and y be the in-plane Cartesian coordinates. Formation of fracture along axis x releases the initially existing thermal bending moment M and causes the fracture edge to rotate through the angle ϑ; see Figure 1b (this figure resembles a situation photographed in the Arctic by *Sanderson* [1988, p. 149, Figure 6.4] and attributed by him to creep buckling; but creep buckling, with fracture, is part of the present model if the elastic modulus is interpreted as the effective modulus for creep, as in equation (25)).

Deflection w in the direction of vertical axis z causes the supporting pressure of seawater to increase by $p = \varrho w$ (Archimedes' law). This means that for one-dimensional response, the plate is exactly equivalent to a beam on Winkler-type elastic foundation whose foundation modulus is exactly equal to ϱ (Figure 1c). The beam is for the time being assumed to carry no axial (in-plane) force. According to *Hetényi* [1946], the edge rotation is given by

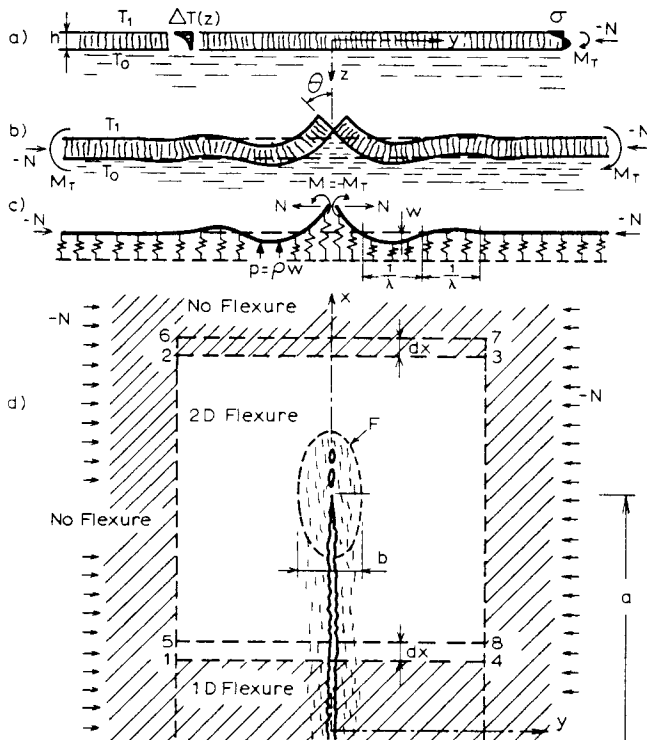$$\vartheta = [w']_{y=0} = \frac{4M\lambda^3}{\varrho} \tag{1}$$

Fig. 1. (a) Floating ice plate, (b) its deformation after fracture, (c) its modeling as a beam on elastic foundation, and (d) view of propagating fracture from top.

where $\lambda = (\varrho/4D)^{1/4}$, with $D = Eh^3/12(1-\nu^2)$ is cylindrical stiffness of the plate, E is Young's elastic modulus of the plate, ν is the Poisson ratio, and the prime denotes derivatives with respect to y. The potential energy release due to fracture, per unit length along the crack, is

$$W = \frac{M\vartheta}{2} = \frac{2M^2\lambda^3}{\varrho} \tag{2}$$

For the sake of simplicity, we will now restrict attention to steady state fracture propagation. This means that the temperature profiles at various locations are approximately the same and the fracture process zone is fully developed and almost constant in size. But it does not mean that the crack velocity should be constant because fracture mechanics is a time-independent theory. Dynamic fracture propagation in which there are significant inertia forces must nevertheless be excluded from consideration. In this regard it may be noted that the inertial forces are negligible for crack tip velocities less than about 0.1 of the speed of sound in ice, which still allows fracture propagation to be quite rapid. (The crack velocities can vary enormously depending on the energy release rate governed by mechanics of the entire structure; see, for example, the observations by *Parsons et al.* [1987] and *Bentley et al.* [1988]).

To isolate the size effect from other effects, only geometrically similar temperature profiles at the fracture front in plates of various thicknesses can be considered. The transients due to temperature changes cannot be considered if the size effect should be mathematically isolated from other phenomena. Creep and time-dependent fracture properties will be taken into account later, and only approximately, using the effective modulus approach, which permits quasi-elastic analysis.

Although the foregoing calculation of energy release is based on analyzing the plate one-dimensionally, as a beam, it applies in general for steady state propagation of a crack. Imagining a view of the sea ice plate from top, one can see a region of progressive crack formation (the microcracked region F centered at the fracture tip in Figure 1d), surrounded by a region of two-dimensional elastic bending of the ice plate (the dashed rectangle 1234 in Figure 1d). Within region F, the fracture progressively grows across the plate thickness, crack bridging may be expected to occur, and the material may be assumed to undergo microcracking in front of the crack. These complex phenomena, however, need not be analyzed because the total energy dissipated in the fracture process zone, representing the macroscopic fracture energy G_f, must be constant by virtue of the assumption of steady state (these phenomena would of course have to be analyzed if we wanted to calculate G_f, but in any case we do not know what material properties to consider for that purpose).

Behind region F, the fracture cuts through the whole thickness h and is opened so widely that there is no crack bridging anymore. The distance of the side 12 or 34 of the rectangle from the crack (Figure 1d) is equal to the reach of nonnegligible bending disturbance due to fracture, which is about $5/\lambda$ (if the amplitude reduction factor $e^{\lambda y} \approx 0.01$ is considered as negligible). In front of the rectangle 1234, the ice plate is undisturbed, and behind the rectangle it is very close to a state of one-dimensional (cylindrical) bending, for which the foregoing calculation applies.

We do not know much about the state of the plate in the region *1234* except for knowing it is very complex. But we do not need to know it if we study only the steady state crack propagation. In that case, if we consider crack extension by dx, the rectangular region *5678* (Figure 1d) obtained by moving rectangle *1234* ahead by dx with the crack advance contains the same amount of energy as the original rectangle. The energy contained within rectangle *2673* (Figure 1d) flows into the rectangle *1234* as it moves forward with the crack, and the energy contained in the rectangle *1584* (Figure 1d) has flowed out. So the overall energy change is given by the difference between the energies contained within the rectangles *2673* and *1584*, and this is exactly what we have calculated.

The energy dissipated per unit length of fracture extension may be expressed as $W = hG_f$, where G_f is the average (mode I) macroscopic fracture energy of the material through the ice plate thickness; $G_f = K_f^2/E$ where K_f is the average (mode I) fracture toughness [*Broek*, 1986] and E is Young's elastic modulus of the ice plate. (The point-wise fracture energy value no doubt strongly varies across the plate thickness because of nonhomogeneity of ice type, brine content, and temperature variation. Note that the average G_f for the thickness of the plate would vary with the thickness of the ice plate if the distributions of the pointwise fracture energy across ice plates of various thicknesses were nonsimilar; this possible effect will be neglected.) Setting $hG_f = W$ (equation (2)), one obtains the following expression for the critical thermal bending moment at which the fracture must propagate:

$$M_f = \sqrt{\frac{\varrho h G_f}{2\lambda^3}} \qquad (3)$$

It must be emphasized that the thermal bending fracture which we are analyzing (Figure 1) does not represent what has usually been understood as the "thermal cracks" in sea ice. These are the cracks whose formation is not associated with plate bending. They could not relieve the bending energy of the plate. They run through only a portion of the plate thickness and their spacing is dense, of the order of 0.5 m.
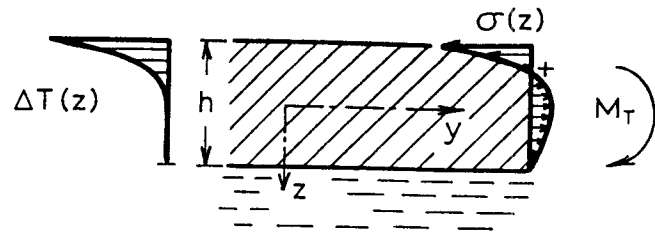

Fig. 2. Profiles of temperature change ΔT, thermal stress σ, and bending moment M_T due to thermal stresses.

4. Critical Temperature Difference and Size Effect

The difference of ice temperature from the temperature of the seawater, T_0, may be written as $\Delta T(z) = \Delta T_1 f(\zeta)$ where z is the vertical coordinate measured from the midthickness of the plate, $\zeta = z/h$ is the relative vertical coordinate, ΔT_1 is the temperature difference between the top and bottom faces of the plate, and f is a function defining the temperature profile (Figure 2), which must be calculated in advance. Taking into account that the normal strains in both the x and y directions as well as the vertical normal stresses are zero, we find that the thermal bending moment in the plate before fracture is

$$M_T = \int_{-h/2}^{h/2} \hat{E}\alpha\Delta T(z)z\,dz \qquad \hat{E} = \frac{E}{1-\nu} \qquad (4)$$

where α is the coefficient of linear thermal expansion of ice [*Anderson*, 1960; *Weeks and Assur*, 1967; *Butkovitch*, 1957] and the value of the elastic modulus E is taken as the average over the plate thickness (which may involve an error similar to that pointed out for G_f). We ignore the variation of α throughout the plate thickness and take an average value. Substituting for $\Delta T(z)$ and denoting $I_T = \int_{-1/2}^{1/2} f(\zeta)\zeta\,d\zeta$ (a constant), we obtain

$$M_T = \hat{E}\alpha\Delta T_1 h^2 I_T \qquad (5)$$

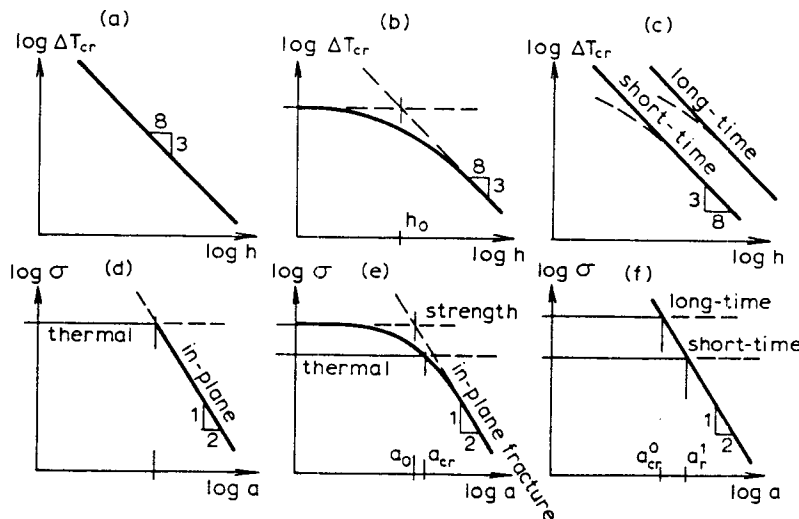Note that the temperature profile $f(\zeta)$ can practically never

Fig. 3. (a) LEFM size effect in thermal bending fracture, (b) deviation from LEFM size effect expected if the fracture process zone is large, (c) difference between short-time and long-time loading due to creep, (d) transition to in-plane fracture with its size effect, (e) size effect in in-plane fracture expected if the fracture process zone is long, and (f) critical crack length for this transition, without and with creep.

become linear except in plates less than about 0.5 m thick. (The depth at which the sinusoidal surface temperature waves of periods 14 days and 1 year get attenuated to $1/e$ of the surface amplitude are 0.97 m and 3.40 m, respectively, according to *Sanderson*, [1988].)

Fracture will propagate if $M_T = M_f$. From this, the critical temperature difference required for crack propagation is

$$\Delta T_{cr} = \Delta T_1 = \frac{1}{\dot{E}\alpha I_T h^2} \sqrt{\frac{\varrho h G_f}{2\lambda^3}} \qquad (6)$$

Substituting now the foregoing expressions for λ and D and rearranging, we obtain the result

$$\Delta T_{cr} = C_1 \, h^{-3/8} \qquad (7)$$

where

$$C_1 = \frac{(1-\nu)^{5/8} \, \varrho^{1/8} \, \sqrt{G_f}}{\sqrt{2} \, [3(1-\nu^2)]^{3/8} \, E^{5/8} \, \alpha \, I_T} \qquad (8)$$

An important aspect to note is that the critical temperature difference depends on h, i.e. there is a size effect (or scale effect). According to plastic limit analysis or elastic analysis with allowable stress, there would be no size effect; i.e., ΔT_1 would be independent of h. The size effect is a basic property of fracture mechanics. For two-dimensional or axisymmetric problems, LEFM predicts the critical stress or critical temperature difference to be proportional to (size)$^{-1/2}$, provided that geometrically similar structures with similar cracks are considered. But in our case (Figure 3a), ΔT_{cr} is proportional to (size)$^{-3/8}$. Why this difference? This is due to the effect of the characteristic length L of decay of bending disturbances along the plate. Because $L = (D/\varrho)^{1/4} = 1/\lambda\sqrt{2} = \propto h^{3/4}$, L increases less than proportionally to thickness h. The width of the strip parallel to crack from which most of the bending energy is released is proportional to L. But to preserve the normal size effect $h^{-1/2}$, this width would have to be proportional to h. Therefore the size effect may be expected to be weaker than $h^{-1/2}$, as we have found.

5. Generalization to Bending Fracture Under In-Plane Forces

In natural conditions, the sea ice plate is normally subjected to a significant in-plane compressive force N, normal to the crack direction (considered negative when compressive). Then, obviously, the second-order geometric effect known from the theory of coumn buckling must be taken into account. Therefore we now generalize the solution to a semi-infinite beam on elastic foundation carrying axial force N. The slope (derivative) w' of the deflection curve $w(y)$ has generally the form [e.g., *Bažant and Cedolin*, 1991, section 5.2]

$$w' = (A \sin ry + B \cos ry)e^{-sy} \qquad (9)$$

where

$$r = \lambda\sqrt{1+\gamma} \qquad s = \lambda\sqrt{1-\gamma} \qquad \gamma = -\frac{N}{2\sqrt{\varrho D}} \qquad (10)$$

and A and B are arbitrary integration constants. The boundary conditions at the free end $y = 0$ are $w' = \vartheta$ (rotation at the crack) and $Dw''' - Nw' = -V = 0$ where the

primes denote derivatives with respect to y and V is shear force in the vertical (z) direction. From these two conditions one solves $B = -\vartheta$ and $A = -\vartheta[s^2 - r^2 - (N/D)]/2rs$. Substituting this into the expression for the bending moment in the beam, which is expressed as $M = Dw''$ after w'' has been calculated by differentiating (9) with respect to y, one obtains (for $y = 0$)

$$M = \frac{1 - 2\gamma}{\sqrt{1-\gamma}} \lambda D\vartheta \qquad (11)$$

The energy release rate due to fracture propagation may be calculated as $W = M\vartheta/2$. Expressing ϑ from (10), we thus get

$$W = \frac{\sqrt{1-\gamma}}{1-2\gamma} \frac{M^2}{2\lambda D} \qquad (12)$$

Setting this equal to the energy dissipated by fracture, $W = hG_f$ and solving for M, one obtains for the critical thermal bending moment M_f causing fracture propagation the result

$$M_f^2 = 2h\lambda DG_f \frac{1-2\gamma}{\sqrt{1-\gamma}} \qquad (13)$$

From the condition that $M_f = M_T$, where M_T is given by (5), it follows that

$$\Delta T_{cr} = \Delta T_1 = \frac{1-\nu}{E\alpha I_T h^2} \sqrt{2h\lambda DG_f \frac{1-2\gamma}{\sqrt{1-\gamma}}} \qquad (14)$$

Finally, introducing the foregoing expressions for λ, D and C_1, and rearranging, one obtains the result

$$\begin{aligned}
\Delta T_{cr} &= C_1 \, h^{-3/8} \, (1-2\gamma)^{1/2}(1-\gamma)^{-1/4} \\
&= C_1 \, h^{-3/8}(1 - \frac{3}{4}\gamma + \cdots)
\end{aligned} \qquad (15)$$

where

$$\gamma = -k_1 \frac{\bar{\sigma}}{\sqrt{h}} \qquad \bar{\sigma} = \frac{N}{h} \qquad k_1 = \sqrt{\frac{3}{E\varrho}(1-\nu^2)} \qquad (16)$$

The last form of (15) has been obtained by Taylor series expansion.

The most interesting aspect of the result in (15) is that the critical temperature difference again exhibits size effect. Asymptotically for small $|N|$ the size effect is the same as before (equation (7)). But as N becomes negative (compressive) of increasing magnitude, the size effect becomes stronger than $h^{-3/8}$, and as N becomes positive (tensile) of increasing magnitude, the size effect becomes weaker. Furthermore, the influence of the average in-plane stress on the size effect diminishes as the plate becomes thicker.

Noting that according to (15) as well as (7) (and for similar temperature profiles), a thicker plate must fracture at a smaller temperature difference, we can explain *Assur's* [1963] observation that new fractures in the arctic pack ice generally do not form along the lines of weakness, such as thin refrozen leads, but run through intact floes and across old pressure ridges. From the strength theory, this observation cannot be explained.

Assur [1963], however, did not explain his observation by thermal stresses; rather, he asserted that these "long-wave cracks," as he called them, "form instantaneously, perhaps connected with a sudden drop in barometric pressure or as

a result of a swell created by a distant storm" [*Assur*, 1963]. This hypothesized explanation, however, has not been analyzed in mechanics terms.

6. Comparison With Strength Theory

For the sake of comparison, assume now that the ice plate follows the strength theory rather than fracture mechanics. Consider that the in-plane force resultant $N_{yy} = N$ in the y direction (Figure 1) is non zero and tensile (normally, of course, the arctic ice plate is under compression, but tensile forces must occur sometimes if openings such as the leads should form). Keeping in mind that the thermal strains occur in both the x and y directions, and assuming that the in-plane force resultants N_{xx} and N_{zz} in both the transverse horizontal and vertical directions x and z vanish, we find that the extreme stress at the tensioned face of the plate is $\sigma_1 = (N/h) + \Delta T \alpha \hat{E}(f_1 - \overline{f})$ where $f_1 = f(\frac{1}{2})$ and $\overline{f}$ is the mean value of the temperature distribution function $f(\zeta)$ in the cross section. Setting the tensile strength of the sea ice material $\sigma_1 = f'_t$ and solving for ΔT, we get

$$\Delta T^\sigma_{\rm cr} = \frac{1-\nu}{\alpha E(f_1 - \overline{f})}(f'_t - \overline{\sigma}) \qquad \overline{\sigma} = \frac{N}{h} \qquad (17)$$

We see that as was mentioned before, this value of the critical temperature difference is independent of the plate thickness h, that is, no size effect exists for the strength theory.

The strength theory, however, could be correct only in the sense of plasticity, in which case the strength is described by the yield condition. Therefore, equation (17) exhibited, after the attainment of the strength (yield) limit, a long yield plateau. But this is not the case for ice. The post-peak softening, characteristic of all quasi-brittle materials, causes localization of strain-softening (damage) zones, and if no localization limiter is included in the mathematical model, the strain-softening damage is predicted to localize into a zone of zero volume (a line or surface). This leads to the absurd conclusion that the failure process would dissipate zero energy [see *Bažant and Cedolin*, 1991, chapter 13, and references therein]. Consequently, the strength theory is not a realistic model for ice, in general. However, studies of the deterministic size effect due to energy release [*Bažant*, 1984; *Bažant and Kazemi*, 1990; *Bažant and Cedolin*, 1991] revealed that the strength theory (or plasticity) should nevertheless provide the correct asymptotic value of nominal strength if the structure size approaches zero.

7. Transition to Fracture Driven by In-Plane Forces

In the foregoing we have tacitly assumed that fracture extension causes no release of the energy of the in-plane forces in the ice plate, in the manner of tensile cracks in a plane. Although the handling of a general in-plane stress state is easy, let us assume that there is no remote shear stress σ_{xy} on the planes parallel to crack direction x. The in-plane remote uniform normal stress in direction y normal to the crack is $\overline{\sigma} = \overline{\sigma}_{yy} = N/h$. The average stress value that would cause the crack in an infinite ice plate to propagate is, according to the well-known Westergaard solution [e.g., *Broek*, 1986],

$$\overline{\sigma} = \frac{\overline{K}_f}{\sqrt{\pi a}} = \sqrt{\frac{E\overline{G}_f}{\pi a}} \qquad (18)$$

in which a is the half length of the crack (Figure 1d); $\overline{G}_f$

is the large-scale fracture energy for in-plane through fracture of the ice plate, which could be much larger than the G_f value for a crack propagating across the plate thickness (bending fracture); and $\overline{K}_f$ is the associated large-scale in-plane fracture toughness. Note that the strength according to (18) is independent of plate thickness.

Equation (18) obviously applies when N is tensile. Typically, though, N is compressive, in which case (18) might at first seem questionable if the ice behavior is pictured exactly as in Figure 1c, which shows no horizontal relative displacement v of the fracture faces. In reality, displacement v must occur not only for tension (Figure 4a) but also for compression (Figures 4b and 4c). The latter case, in theory, implies an overlap of the fracture faces (Figure 4b), which would of course be physically impossible. But in reality, the fracture faces are weakened by the microcracking that has occurred in the fracture process zone of thermal fracture. It must therefore be expected that the fracture faces undergo crushing, which is the mechanism leading to pressure ridge buildup. Alternatively, even if the ice has not been sufficiently weakened, the contact of the plate corners pictured in Figure 1b is an unstable situation and the loss of stability must lead to the slipping of one plate under the other (rafting), as shown in Figure 4c. This again produces a horizontal displacement v (although in combination with vertical relative displacement of fracture faces, which causes post-thermal-fracture bending of the ice plates but not their in-plane behavior, and is therefore ignored here). So we conclude that (18) applies, at least approximately, even for compression.

Note that if there were no crushing and no rafting, as pictured in Figure 1b, then the compressive force N would have the effect of diminishing the energy release since the location of N would shift downwards toward the corner point (Figure 1b). This would cause N to do additional work on the horizontal displacement $v_1 = -\vartheta e$ where ϑ is the cross section rotation at the fracture face (Figure 1b) and e is the downward shift (or eccentricity) of force N after fracture (Figure 1c). This effect would tend to increase the critical
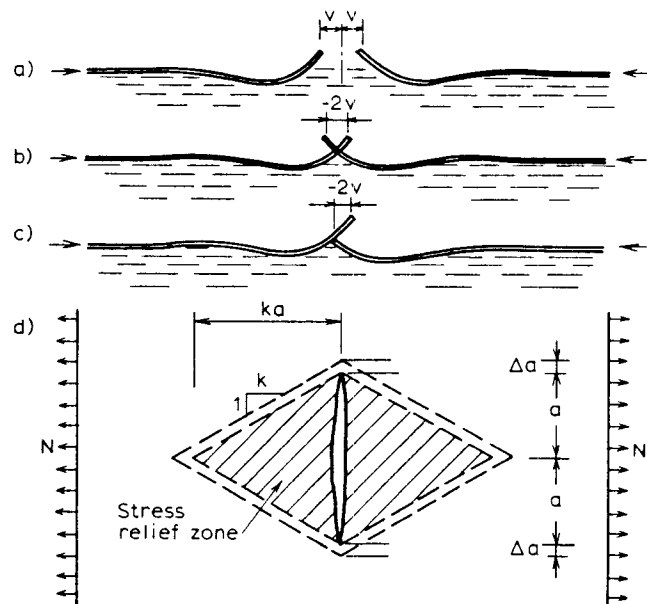
Fig. 4. Horizontal displacement of fracture faces: (a) opening in tension, (b) crushing in compression, and (c) rafting in compression; and (d) stress relief zone of in-plane forces, viewed from top.

temperature difference. But it seems unrealistic in view of the likelihood of compression crushing or rafting.

Now consider the size effect. According to (18), $\overline{\sigma} \propto a^{-1/2}$. In the plot of $\log \overline{\sigma}$ versus $\log a$ (Figure 3d), equation 18 yields a straight line of slope -1/2, which represents the same size effect as for any solution of two- or three-dimensional solution of (LEFM) (by contrast, according to a strength criterion or plasticity, $\overline{\sigma}$ would exhibit no size effect). In the plot of Figure 3d, thermal bending fracture is represented by a horizontal line, since the crack length a does not appear in equation (7). Obviously, these two straight lines intersect at a certain critical crack length

$$a_{\mathrm{cr}} = \frac{E\,\overline{G}_f}{\pi\,\overline{\sigma}^2} \qquad (19)$$

Now it may be noted that $\overline{\sigma}$ is basically controlled by the mechanism of ice floe movements in the Arctic Ocean and is basically independent of the thermal effects. It follows that the fracture formation and growth is driven by thermal bending only at the beginning. When the crack becomes long enough, namely,

$$a > a_{\mathrm{cr}} \qquad (20)$$

the thermal stresses must cease to matter and the fracture becomes driven by in-plane forces. Steady state propagation of thermal bending fracture can go on ad infinitum only when the in-plane force happens to vanish, $N = 0$, which is an unlikely situation. For $N \neq 0$, the propagation can be only quasi-steady, up to fracture length a_{cr}.

Intuitive understanding of the size effect of a is helped by realizing that formation of a crack of length a relieves the stress approximately from the triangular zones shaded in Figure 4d [Bažant, 1984; Bažant and Cedolin, 1991, chapters 12 and 13]. Their combined area is $A_e = 2ka^2$, where k is a constant representing the slope shown in the figure. Before fracture, the strain energy density is $\overline{\sigma}^2/2E$. The total energy release due to formation of a crack of length a is $W = hA_e\overline{\sigma}^2/2E = 2hka^2\overline{\sigma}^2/2E$. The energy release rate must be equal to $\overline{G}_f h$, i.e., $\partial W/\partial a = 2hk\overline{\sigma}^2 a/E = \overline{G}_f h$. From this, the stress required for crack propagation is $\overline{\sigma} = (E\overline{G}_f/2ka)^{1/2}$. This is now seen to coincide with (18) if one sets $k = \pi/2$.

In words, the reason for the size effect of a is that for a longer crack the energy release per unit crack extension ($\Delta a = 1$) comes from a larger area (the four white strips around the triangular zones in Figure 4d). Therefore the energy density in this area, and thus also the stress, must be smaller, so that the energy release per unit crack extension would be the same for any crack length.

By a similar argument one can also explain why there is no size effect of crack length in the thermal bending fracture. The zone of (partial) relief of thermal stress is the white rectangular zone 1234 in Figure 1d (which extends to the distance $5/\lambda$ to each side of the crack). By contrast to the previous case, the size of this zone does not change with the crack length (if a is already longer than the length of the fracture process zone, 12 in Figure 1d).

8. Spacing of Parallel Cracks

Consideration of the stress relief zones makes it also possible to estimate the minimum spacing $s_{\min}$ of parallel cracks in the ice plate. If the stress relief zones of two adjacent cracks overlap, the energy release available for driving each

crack diminishes. So the minimum spacing is roughly given by the condition that the stress relief zones of parallel cracks do not overlap. Thus we obtain the following two conditions:

Thermal fracture $\qquad s_{\min} \approx 10/\lambda \qquad (21)$

Fracture driven by $N \qquad s_{\min} \approx 2ka = 4\pi a \qquad (22)$

The former condition will dominate for a short enough crack, and the latter condition will dominate for a long enough crack. Two parallel thermal cracks may form at their minimum spacing, but as they become long enough for the second condition to govern, one of them must get arrested and close. More likely, though, since the G_f values at the location of two potential adjacent cracks will differ, because of the randomness of ice, the adjacent thermal crack might not form at all before the second spacing condition starts to govern, and then the spacing can be much larger than the thermal $s_{\min}$ already from the beginning.

Equation (22) can explain why the spacing of new fractures in sea ice plates is usually much larger than indicated either by the present thermal bending fracture analysis or by strength considerations. The latter [Evans, 1971] provided the estimate $s_{\min} = 200$ m, which appears to be much too small.

9. Effect of Large Fracture Process Zone and Deviations from LEFM

It has already been pointed out that the length L_f of the fracture process zone F in ice is likely to be an order of magnitude larger than the size of the dominant material inhomogeneities, which are represented by the brine pockets and the blocks between adjacent preexisting thermal cracks (about 0.5 m). In plate bending there are further influences. The plate bending theory is invalid at distances that do not exceed at least several times the plate thickness h. Also, L_f must exceed the length over which the vertical bending crack grows across the full thickness of the plate, which is again likely to be at least several times the plate thickness. Therefore, as a crude, order-of-magnitude estimate, $L_f \approx 10h$.

Much has recently been written about the size effect in structures with a large fracture process zone. It impossible to reproduce the detailed arguments (see, for example, chapters 12 and 13 in the textbook of Bažantand Cedolin [1991]). Suffice it to say that, as a result of crack tip blunting and shielding by the process zone, the size effect must be transitional between plasticity and LEFM. This is described by the curve in Figure 3b, which replaces the plot in Figure 3d. The horizontal asymptote in Figure 3a corresponds to a solution according to plasticity (strength criterion), and the inclined asymptote of slope -1/2 to a solution according to LEFM. Based on the approximate theory explained by Bažant and Cedolin [1991], the transitional size effect corresponding to this curve is reasonably described by the following approximate generalization of equation (18)

$$\overline{\sigma} = \sqrt{\frac{E\overline{G}_f}{\pi a}}\left(1 + \frac{a}{d_0}\right)^{-1/2} \qquad (23)$$

where d_0 is an empirical constant, whose order of magnitude is $10L_f$. For $a \gg d_0$, this equation becomes identical to (18), while for $a \ll d_0$ there is no size effect, as in plasticity.

One consequence is a decrease in the value of a_{cr}, beyond which the fracture driven by in-plane forces begins to dom-

inate. Instead of Figure 3d, this value is obtained as the intersection point of the dashed horizontal line for thermal fracture with the size effect curve, as shown by the a_{cr} value shown in Figure 3e.

Another consequence is a modification of the effect of plate thickness h. For a thin enough plate that is not much thicker than the size of ice inhomogeneities, there should be no size effect. This means that the plot of $\log \Delta T_{cr}$ versus $\log h$ should look as shown by the curve in Figure 3b. This curve asymptotically approaches the straight line of slope -3/8 which corresponds to equation (6) or (15).

A further consequence of a large fracture process zone is that the LEFM-based apparent fracture energy required for crack growth increases as the crack grows. The law describing this growth is called the R curve. A method to determine the R curve from the size effect on maximum loads is available [e.g., *Bažant and Kazemi*, 1990]. The transitional size effect implies R curve behavior.

In view of the experience with other heterogeneous materials such as concrete, rock, and ceramics, it is possible that the effective value of fracture energy to be used in bending fracture analysis is not a constant, as is assumed in LEFM, but increases with the plate thickness h until, beginning with a certain thickness, a constant asymptotic value G_f is reached. This increase, which is explained by an increase in the fracture process zone size, would cause the size effect plot of $\log \Delta T_{cr}$ versus $\log h$ to change from a straight line of slope -3/8 (equation (7) or (15); Figure 3a) to the curve sketched in Figure 3b, asymptotically approaching toward the left a horizontal line and toward the right the inclined straight line. In analogy to the theory first expounded for concrete [*Bažant and Cedolin*, 1991, chapters 12 and 13], an approximate equation for this line may be obtained by replacing (in equation (7) or (15)) h with $h + h_0$ where h_0 is an empirical constant; this transforms (7) into

$$\Delta T_{cr} = C_1(h_0 + h)^{-3/8} \qquad (24)$$

This equation approaches (7) when $h \gg h_0$.

10. Effect of Heterogeneity and Temperature Profile

Sea ice plates are highly inhomogeneous, not only because of their columnar microstructure and presence of voids, brine pockets, and larger blocks delineated by weak interfaces (such as partially refrozen thermal or other cracks, or just layers of weaker ice), but also because the ice properties vary through the plate thickness. This variation is of twofold origin: (1) The size of columnar crystals, as well as the size of voids or brine pockets, varies with the depth, and (2) the temperature, which affects the mechanical properties of sea ice to a major extent, varies with the depth and remains equal to the water temperature and the bottom of the plate. The variation of the elastic properties across the plate thickness was not considered in the analysis; however, the present analysis remains applicable if the E modulus is interpreted as the proper weighted average of the actual values of E moduli over the plate thickness. If the relative distribution of the E modulus over the thickness is approximately the same for various thickness values, then the foregoing conclusion about the size effect remains true.

It might also be thought that the vertical shift of neutral axis of bending due to inhomogeneity across the plate thickness causes the in-plane force N to produce a bending moment. In reality, however, such a bending moment cannot exist because the average curvature over long distances must remain zero. Thus the in-plane force resultant N must coincide with the shifted neutral axis, except near a local disturbance, such as that analyzed in this paper.

The foregoing analysis implies the temperature profiles for various plate thicknesses to be similar. That is attainable if the prior temperature histories and the times of prior temperature exposure scale as the square of the plate thickness. The occurrence of such conditions in nature is one chancy event among infinitely many. A lack of profile similarity would of course engender deviations from the presently derived size effect. But, as was already remarked, without profile similarity many effects are mingled together with the size effect and it is impossible to say what the size effect is. It will be necessary to consider similar profiles if the size effect should be brought to light.

11. Effects of Creep and Crack Propagation Speed

The foregoing analysis has neglected creep, which is very strong in the case of ice. Owing to heat conduction, the temperature changes can occur only over a finite period of time, and so creep is always present.

One effect of creep is to relax thermal stresses. In the context of the quasi-elastic analysis performed here, the relaxation of thermal stress due to creep of ice can be approximately taken into account by replacing the value of elastic modulus E in equation (4) with the effective (sustained) modulus $E_{eff} = E/(1 + \varphi_t)$, where E represents the secant modulus for rapid (nearly instantaneous) loading (see the creep isochrones in Figure 5) and φ_t is the creep coefficient, representing the ratio of creep-to-elastic strains for the typical duration t_1 of the temperature difference in the plate; see Figure 5. Because of the pronounced nonlinearity of the creep strain as a function of stress σ (Figure 5), the value of this ratio varies through the thickness of the plate as well as along the plate. For the sake of simplicity we assume that we can approximately take a certain average value of φ_t, determined as the creep-to-elastic strain ratio for a certain average stress level σ_0; then, with reference to Figure 5, $\varphi_t = \epsilon_t/\epsilon_0$ where ϵ_0 is the instantaneous strain and ϵ_t is the creep strain.
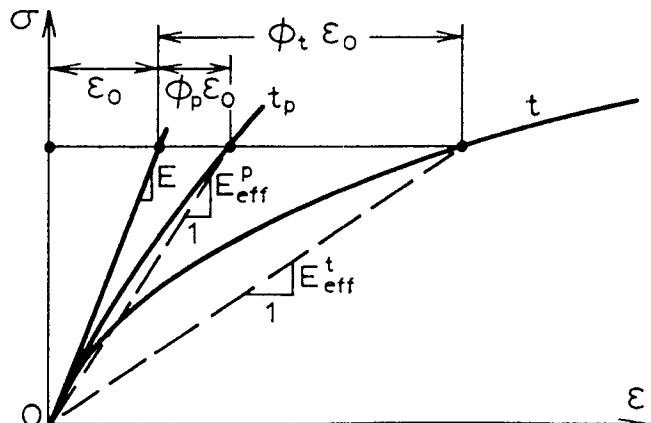

Fig. 5. Creep isochrones of ice and effective moduli for quasi-elastic analysis.

Another effect of creep is to reduce the energy release due to crack propagation. Let t_p be the time that the fracture process zone (the oval-shaped zone F in Figure 1d) takes to travel across a fixed point (this time is not shorter than the time the crack takes to spread vertically through the whole thickness of the plate, and is longer the thicker the plate). Noting that the value of the cylindrical stiffness D is proportional to E, we can take creep approximately into account by replacing D in equation (13) with $D/(1 + \varphi_p)$ where φ_p is the creep coefficient representing the value of the creep-to-elastic strain ratio for the time duration t_p (Figure 5). Again, owing to nonlinearity of the creep law of ice, this ratio varies through the plate thickness and along the plate but, for the sake of simplicity, is taken as a constant, evaluated for the average stress level σ_0.

One may now retrace the foregoing derivation of equations (7) and (15), replacing E with the effective moduli for creep as indicated above. This shows that (7) and (15) remain valid but the expressions for C_1 given in (8) and for k_1 in (16) must be modified as follows:

$$C_1 = \frac{(1-\nu)^{5/8}\varrho^{1/8}\sqrt{G_f}}{\sqrt{2}\,[3(1-\nu^2)]^{3/8}\,I_T\,E^{5/8}\alpha}\,\frac{1+\varphi_t}{(1+\varphi_p)^{3/8}} \qquad (25)$$

$$k_1 = \sqrt{\frac{3\,(1-\nu^2)}{E\,\varrho}}\,(1+\varphi_p) \qquad (26)$$

We see that the creep prior to fracture, which relaxes the thermal stresses, tends to increase ΔT_{cr}, while the creep during fracture, which reduces the energy release rate, tends to decrease ΔT_{cr}. The latter effect, however, is (for the same amount of creep) milder, due to the exponent $\frac{3}{8}$.

Now let us discuss the typical magnitudes of the creep coefficients. The crack propagation seems to be usually very fast [Assur, 1963], with the distance of about a hundred meters traversed in perhaps less than a second. Even if it is less than an hour, the creep coefficient φ_p is very small compared with 1. Therefore one can probably set $\varphi_p \approx 0$ in most circumstances. This also means that γ is almost unaffected by creep.

On the other hand, the duration of a significant temperature difference across the thickness of the plate is quite long, although not more than the duration of the cold season of the year. Thus φ_t could be quite large. However, since the energy available to drive the crack propagation declines with time as the thermal stresses develop and relax, the crack, if it forms and propagates at all, must do so right after heat conduction spreads the temperature change throughout the plate thickness and produces a significant thermal bending moment. Thus time t_1 roughly represents the half-time of the heat conduction process across the thickness of the plate, which is proportional to the square of thickness, i.e., h^2. This halftime may perhaps be estimated as several weeks for a typical plate thickness. For such a duration of thermal stresses, the creep is quite significant, and the effective value of φ_t may be expected to exceed 1.

The fracture propagation rate has still another effect: The slower the crack propagation, the smaller is the effective value of the fracture energy, G_f [e.g., Schapery, 1989]. This is caused by the random distribution of thermal vibration energies of molecules, particularly the fact that the longer the stress duration, the higher the probability that this energy exceeds the activation energy barrier for intermolecular bond breakage. This effect, however, seems unimportant for the present problem because the typical crack propagation speed is probably of the same order of magnitude in most situations.

According to equation (25) with (15) or equation (7), the critical temperature difference ΔT_{cr} necessary for crack propagation should increase as the duration of development and relaxation of the thermal stresses increases. Since this duration is longer for a thicker ice plate, ΔT_{cr} is magnified by creep in a thicker plate more than in a thinner one. This offsets to some extent the size effect given by $h^{-3/8}$.

Indirectly, the creep also affects the transition to nonthermal fracture propagation driven by in-plane forces. Considering that φ_p is either negligible or constant, as already explained, the value of C_1 increases for a longer duration of thermal stresses. The result is that the inclined straight line in the size effect plot in Figure 3c is pushed to the right. At the same time the value of the critical crack length according to (19) is basically constant (E in this equation needs to be replaced by $E/(1+\varphi_p)$ but $\varphi_p \approx 0$). Thus for a longer duration of thermal stresses, the transition from thermal bending fracture to non-thermal in-plane fracture takes place at a shorter critical crack length a_{cr} (Figure 3f). Furthermore, since the thermal stress duration is in a thicker plate longer, this indirectly also causes a_{cr} to be larger for a thicker plane, compared with the elastic solution without creep.

The foregoing approximate consideration of creep is, admittedly, rather crude. A more realistic numerical analysis would of course be possible using finite elements and small time steps. But such an approach would obscure the basic trends and influences that have been brought to light by the present simplified analytical solution.

12. Numerical Estimates

To gain some idea of what this theory predicts, consider the following typical values of material parameters: $\varrho = 9810$ N m^{-3}, $\nu = 0.29$, $\alpha = 5\times10^{-5}\,^{\circ}$C^{-1} (according to Weeks and Assur [1967] and Butkovich [1957]) (the foregoing α value applies only under -10°C; for higher temperatures α varies strongly with temperature and ice salinity and reaches high negative values close to the melting point). The value of the truly instantaneous elastic modulus E_0, inferred from the velocity of high frequency sound waves, is $E_0 \approx 7$ GPa. For our simplified analysis, however, we need to include the primary (short-time) creep into the apparent elastic (short-time) deformation, which means that we need to use for E the apparent elastic modulus value obtained in conventional static tests in laboratory testing machines, approximately $E = 1$ GPa (the same value as used in the thermal cracking analysis of Evans [1971]). According to Urabe and Yoshitake [1981], Weeks and Mellor [1984], and Sanderson [1988, p. 91] we will use for fracture toughness of sea ice the value $K_f = 0.1$ MN m$^{-3/2}$. The corresponding fracture energy value is $G_f = K_f^2/E = 10$ N m^{-1} (as already pointed out, the actual effective value for large-scale fracture of ice plates might be rather different, due to the increased process zone size and the effect of large inhomogeneities, but there are no test data in this regard and theoretical speculations based on micromechanics methods are beyond the scope of this paper). The value 10 N m^{-1} is roughly 100 times larger than

the (thermodynamic) surface free energy of ice [*Ketcham and Hobbs*, 1969].

To take creep into account, we need to estimate at least roughly the average magnitude of thermal stresses. If the primary creep is assumed to be approximately included in the apparent elastic compliance $1/E$, and if the secondary creep is taken into account using Norton's law, the stress-strain relation may be approximately written as

$$\frac{d\epsilon}{dt} = \frac{1}{E}\frac{d\sigma}{dt} + k_c\sigma^3 \qquad (27)$$

where t is time and $k_c = Ae^{-Q/RT}(1 - \sqrt{v_b/v_0})^{-3}$ [*Sanderson*, 1988, p. 82], in which Q is activation energy of creep, R is gas constant, $Q/R = 7818$ °K, $A = 3.5 \times 10^6$ MPa^{-3} s^{-1}, $v_0 = 0.16$, and v_b is the porosity due to brine pockets, which we take as $v_b = 0.06$. Considering temperature $-40°C$, i.e., $T = 233°K$, we get $k_c = 161 \times 10^{-9}$ MPa^{-3} s^{-1}.

Suppose now that a dramatic temperature drop of $\Delta T = 40°K$ occurs over the period $\Delta t = 14$ days. According to the effective modulus method, the creep value may be approximately based on the final stress σ. To get its crude estimate, we may write for uncracked ice at the top plate surface an incremental uniaxial stress-strain relation,

$$\frac{\sigma}{E} + k_c\sigma^3\Delta t = \alpha\Delta T \qquad (28)$$

Substituting the aforementioned values and solving this cubic equation for σ, we get the estimate $\sigma = 0.209$ MPa, which compares well with recent in situ measurements [*Johnson et al.*, 1985; *Tucker and Perovich*, 1991]. The basic equation of the effective modulus method is $\epsilon = \sigma/E_{\text{eff}}$ with $E_{\text{eff}} = E/(1 + \varphi_t)$ and $\epsilon = \alpha\Delta T$. From this we solve $\varphi_t = (E\alpha\Delta T/\sigma) - 1 = 8.57 \approx 9$.

To estimate the value of I_T, we assume the characteristic temperature profile to be a cubic parabola with a zero slope at the bottom of the plate, for which one obtains $I_T = 3/40$. As for the value of h_0 for (24), we neglect it for lack of information. So we use (7) with (25), which then yields the following estimates (plotted in Figure 6):

$$
\begin{aligned}
h &= 1\text{m} & \Delta T_{\text{cr}} &= 24.6°K \\
h &= 3\text{m} & \Delta T_{\text{cr}} &= 16.3°K & (29) \\
h &= 6\text{m} & \Delta T_{\text{cr}} &= 12.6°K
\end{aligned}
$$

These values are frequently exceeded by the arctic weather. This implies that thermal bending moments are indeed capable of causing a bending fracture through the whole thickness of the ice plate. Because of the simplifying hypotheses made and the uncertainty of the input values, however, this result is not a proof of the hypothesis of thermal bending fracture. A proof would require extensive measurements and some sophisticated computer analysis, such as the finite element analysis with a realistic model for the material behavior in the fracture process zone.

The minimal spacing of the through-the-thickness thermal bending cracks obtained from (21) is $s_{\min} = 240$ m for $h = 1$ m, 316 m for $h = 3$ m, and 376 m for $h = 6$ m. These values are close to the estimate of *Evans* [1971] made on the basis of strength theory. Note that this spacing is much larger than the spacing of the thermal cracks in the surface layer,
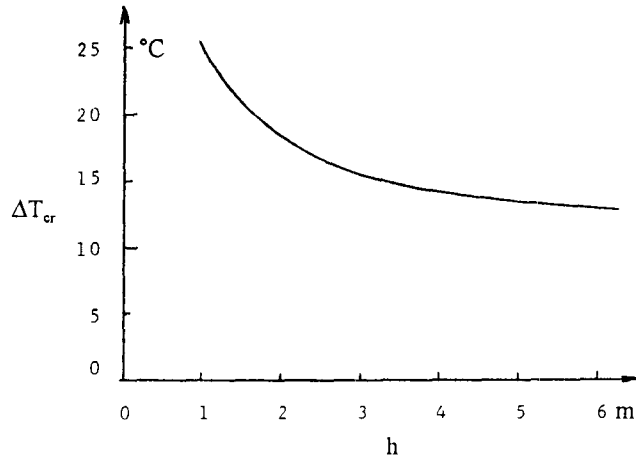

Fig. 6. Dependence of the critical temperature difference required for thermal bending fracture on the ice plate thickness.

which is known to be about 0.5 m and occurs independently of bending.

The fracture energy value used above is no doubt only a crude guess. Based on the recent intensive studies of other quasi-brittle materials such as concrete, rocks, and modern toughening ceramics, it is not inconceivable that G_f could be 1 or 2 orders of magnitude larger than the fracture energy value observed in the laboratory specimens of usual size. The reason is that the G_f value needed for the present purposes must lump the fracture energies dissipated by all the microcracks across the full width b (Figure 1d) of the fracture process zone. In that case the value of ΔT_{cr} would be 3 to 10 times larger. Such large temperature differences could not occur in nature, and in that case the present hypothesis of thermal bending fracture would be invalidated.

On the other hand, because the cracks in the fracture process zone are likely to pass predominantly through the surfaces of weakness, such as the preexisting (perhaps partially refrozen) cracks, voids, and brine pockets, the effective G_f value could also be about equal to the value measured on the laboratory specimens (as we assumed in our calculations), or even substantially less than that. Measurements in the Arctic, as well as sophisticated micromechanics modeling of sea ice behavior in the fracture process zone, are certainly needed to resolve this question.

For the strength theory, *Evans* [1971] used the tensile strength of the ice plate $f'_t = 0.6$ MPa (although for large-scale rupture of ice plates a much smaller value might be appropriate). Assuming, for example, that $N/h = 0.2$ MPa (tension), (17) yields $\Delta T_{\text{cr}}^\sigma = 4.26°K$, independently of plate thickness.

As an example of the transition length calculation, consider that $\overline{G}_f \approx 1000 G_f \approx 10,000$ N m^{-1} and $N/h = 0.03$ MPa ($= 5\%$ of the strength limit). For this case, equation (19) yields $a_{\text{cr}} = 3500$ m. But if $\overline{G}_f \approx G_f \approx 10$ N m^{-1}, then $a_{\text{cr}} = 3.5$ m, in which case the transition to fracture dominated by in-plane forces would occur right at the beginning (in this case the only possible role of the thermal bending fracture would be to trigger the propagation of the in-plane fracture; but if at the same time $N/h = 0.5\%$ of the strength limit, then $a_{\text{cr}} = 350$ m, which means that the thermal bending would dominate at the beginning of propagation). Unfortunately, at present there are order-of-

magnitude uncertainties about the material properties to use as input in these calculations. Further research is needed.

If we would not want to study size effect, other temperature profiles could be examined. Consider for example parabolic profiles that are identical in z and have the penetration depth of 1 m regardless of h ($h \geq 1$ m), while $\Delta T = 0$ below 1 m depth. For $h = 1$ m, 3 m, and 5 m, one would then get $I_T = 1/12$, 5/108, and 11/432, respectively. Equation (7) with (25) would then yield $\Delta T_{cr} = 22.1°$K, 26.4°K, and 37.1°K, respectively. So in this case the thickest plate would be the least likely to fracture. But if cooling continues, the temperature profile in the thickest plate will reach deeper, bringing this plate closer to the point of fracturing, while in the thinnest plate this trend does not happen.

The last observations suggest another viewpoint: Let us consider for each plate thickness such a profile that maximizes the chance to fracture, i.e., minimizes the value of ΔT_{cr}. According to (7), (8), and (15), this happens when I_T is maximized. Considering the temperature history to be a step function, the temperature profile according to the heat conduction equation is approximately parabolic up to the penetration depth $\delta(t)$, below which $\Delta T = 0$; $\delta(t) = \sqrt{12 C_T t}$ where C_T, heat conductivity in ice, is constant. Calculating I_T for a general $\delta(t)$ and setting $dI_T/d\delta = 0$, we find that the maximum I_T occurs at time t when $\delta(t) = h$, i.e., when the cooling front has just reached the plate bottom, regardless of thickness h. For that case we get $I_T = 1/12$. But this is only slightly more that the value 3/40 we considered before. Thus the ΔT_{cr}-values we obtained before are nearly the smallest critical temperature drops possible.

Now an important point to note is that although the most critical temperature profiles for plates of various thicknesses occur at different times t, they are similar. This is another argument in favor of the assumption of similar profiles. It is exact, however, only if creep is ignored. If creep is taken into account, then (according to (25)) the critical temperature profile occurs at time t when the value of $I_T[\delta(t)]/\varphi_t$ is maximized, and this no longer yields similar profiles.

13. Method to Identify Material Parameters

Having a suitable theory, observations of the formation of large fractures on the Arctic Ocean could be exploited for obtaining the values of the basic parameters in the present model, particularly the fracture energy for large scale fracture. This approach, however, can succeed only if the current ice conditions and their history prior to fracture are carefully documented, especially the history of air temperature and the history of ice thickness. From such data and the known value of thermal conductivity (about 1.15×10^{-6} m² s⁻¹ [Sanderson, 1988]) the histories of temperature profiles as well as salinity profiles can be deduced by solving the appropriate diffusion equations.

The simplified analytical formulation presented here would no doubt be too crude for this purpose (except for order-of-magnitude estimates of the fracture energy value). It would be necessary to develop a nonlocal finite element or boundary element code with step-by-step integration in time. Having all the information, and taking creep carefully into account (including the effects of time variable stress, temperature and salinity at various points of ice), it would

be possible to calculate with reasonable accuracy the thermal stresses that must have existed just before the observed fracture formation. Some estimate of the in-plane force N just before fracture formation would have to be also made (probably by some on-site invasive measures). Then it would be possible to calculate the energy release caused by fracture formation, from which the effective value of fracture energy for the bending fracture mode of an ice plate of realistic thickness would follow. Of course, a considerable code development effort and computer power would be needed for such an undertaking.

14. General Proof of (−3/8) Power Size Effect

Finally, since the thermal fracture can be of finite length a and can be curved, it is interesting to examine whether the $h^{-3/8}$-size effect holds in general. The governing differential equation for the two-dimensional deflection surface $w(x, y)$ is $D\nabla^4 w + \varrho w = 0$. The plate is infinite, with the boundary condition $w = 0$ at infinities. At the crack faces Γ, which can now be curved, the boundary conditions are $Dw_{,nn} = M_T$ and $w_{,nnn} + (1 - \nu)w_{,ntt} = 0$, where subscripts following a comma denote partial derivatives, and n and t are the coordinate axes normal and tangential to the crack face. Introduce now dimensionless variables $\xi = x/L$, $\eta = y/L$ and $\zeta = w/L$, where $L =$ decay length $= (D/\varrho)^{1/4} = 1/\lambda\sqrt{2}$, and note the transformation of derivatives: $\partial/\partial x = L^{-1}\partial/\partial\xi$, etc. Transforming the boundary value problem to these variables, we have the governing partial differential equation

$$\nabla^4 \zeta + \zeta = 0 \qquad (30)$$

with boundary conditions $\zeta = 0$ at infinities, and, at crack faces Γ_0 in dimensionless coordinates:

On Γ_0 $\zeta_{,\nu\nu} = \dfrac{L}{D} M_T$ $\zeta_{,\nu\nu\nu} + (1 - \nu)\zeta_{,\nu\tau\tau} = 0$ (31)

where ν and τ are the coordinate axes normal and tangential to the crack faces Γ_0 in the dimensionless space (ξ, η).

Owing to linearity of (30) and (31), the solution ζ is proportional to M_T. Therefore, it is convenient to define: $\zeta = F(\xi, \eta; \bar{a}) =$ solution of differential equation (30) for the relative crack length $\bar{a} = a/L$ and for the aforementioned boundary conditions except that the first boundary condition in (31) is replaced by $\zeta_{,\nu\nu} = 1$. In this boundary value problem, there are no physical constants, and so the solution F is independent of size and material properties, and depends only on $\bar{a}$. Then the solution for the actual boundary conditions (31) is

$$\zeta = \frac{L}{D} M_T F(\xi, \eta, \bar{a}) \qquad (32)$$

Now, by transformations of coordinates, we have, on the crack faces Γ, $\zeta_{,\nu} = F_{,\nu} M_T L/D, \zeta_{,n} = \zeta_{,\nu}/L$, and $\vartheta = w_{,n} = L\zeta_{,\nu} = F_{,\nu} M_T L/D =$ rotation at the crack face about the tangential axis τ. The total complementary energy release due to fracture, Π, is equal to the work of the released thermal bending moment, as it is reduced to zero, on rotation ϑ, i.e. $\Pi = \int_a \frac{1}{2} M_T \vartheta \, da$. From this, the energy release per unit length of fracture, $\partial\Pi/\partial a = \frac{1}{2} M_T \vartheta = G_f h$. Substituting now the foregoing expression for ϑ, solving the resulting

equation for M_T, and expressing M_T in terms of ΔT_{cr} (equation (5)), and L and D in terms of h, we obtain the following result, in which C_1 is the same as in equation (8);

$$\Delta T_{cr} = \frac{2^{1/4}(1-\nu)^{3/8}}{\sqrt{F_{,\nu}(\xi,\eta;\bar{a})}}\, C_1\, h^{-3/8} \qquad (33)$$

This proves in general that thermal bending fracture of floating ice plate exhibits a $(-3/8)$-power size effect, provided that either F is independent of the crack length (as in our previous problem) or the crack length a is proportional to the decay length L (rather than to thickness h). The last condition ought to be satisfied at least asymptotically for $h \to \infty$. Indeed, if it were not satisfied, a would be proportional to L^q where $q \neq 1$; but then the crack length could become either much larger or much smaller then than the decay length L, both of which are implausible (unless F is independent of a, as in our problem).

It is interesting to express the size effect in terms of the decay length L. Because $h \propto L^{4/3}$, equation (33) implies that

$$\Delta T_{cr} \propto L^{-1/2} \qquad (34)$$

Thus in terms of the decay length of the floating plate, we have the standard size effect of linear elastic fracture mechanics. In the case of cracks of finite length, this size effect is again applicable only to cracks whose length is proportional to L, not h. This simple conclusion is not surprising since the plate problem is two-dimensional, and, in the plane (x,y), length L is the only characteristic length present in the problem (h enters only indirectly, through D).

15. Conclusions

1. Quasi-elastic analysis based on plate bending theory indicates that release of the bending energy of the plate with a thermal gradient could possibly be the cause of the sudden formation of long, through-the-thickness fractures in Arctic plate ice, cutting through thick intact portions of ice floes. However, because of crude simplifying hypotheses of the analysis, as well as the uncertainty of the large-scale material properties required as the input, the analysis does not prove that this is actually the case.

2. If steady state propagation of through-the-thickness thermal bending fracture along a sea ice plate indeed takes place, it must exhibit a size effect, such that the critical temperature difference between the top and bottom of the plate causing fracture propagation decreases with an increasing plate thickness.

3. For the case that the in-plane normal force is negligible, linear elastic fracture mechanics shows that the critical temperature difference required to produce the thermal bending fracture (if it exists) is proportional to (thickness)$^{-3/8}$.

4. For the case that the in-plane forces are significant, fracture mechanics shows that, beyond a certain critical crack length, the thermally driven bending fracture (if it exists) must change to a planar (nonflexural) fracture driven by the release of the energy of the in-plane forces (generated by wind and ocean currents) rather than the energy of the thermal stresses.

5. The effect of creep is to increase the critical temperature difference required to produce the bending fracture (if it exists), as well as the critical crack length for the transition to in-plane fracture.

6. The presently advanced hypothesis of thermal bending fracture cannot be proven or disproven without new types of experiments and measurements in the Arctic and their computer modeling.

REFERENCES

Anderson, D.L., The physical constants of sea ice, *Research, 13,* 310–338, 1960.

Assur, A., Breakup of pack-ice floes, in *Ice and Snow: Properties, Processes and Application,* MIT Press, Cambridge, Mass., 1963.

Bažant, Z.P., Size effect in blunt fracture: Concrete, rock, metal, *J. Engrg. Mech., 110,* 518–535, 1984.

Bažant, Z.P., Large-scale fracture of sea ice plates, *Proc. 11th IAHR Intern. Symp.* (held in Banff, Alberta, Canada), University of Alberta, Edmonton, 991–1005, 1992.

Bažant, Z.P., and M.T. Kazemi, Size effect in fracture of ceramics and its use to determine fracture energy and effective process zone length, *J. Am. Ceram. Soc., 73(7),* 1841–1853, 1990.

Bažant, Z.P., and L. Cedolin, *Stability of Structures: Elastic, Inelastic, Failure and Damage Theories,* Oxford University Press, New York, 1991.

Bažant, Z.P., and J.-K. Kim, Fracture theory for nonhomogeneous brittle materials with application to ice, in *Proceedings, ASCE National Conference on Civil Engineering in the Arctic Offshore – ARCTIC 85,* edited by L.F. Bennett, pp. 917–930, ASCE, New York, 1985.

Bažant, Z.P., and Y. Xi, Statistical size effect in quasibrittle structures, II, Nonlocal theory, Report, Dep. of Civ. Engg., Northwestern Univ., Evanston, IL, 1990. (Also *ASCE J. Engg. Mech., 117(11),* pp. 2623-2640, 1991.)

Bentley, D.L., J.P. Dempsey, D.S. Sodhi, and Y. Wei, Fracture of S2 columnar freshwater ice, Floating double cantilever beam tests, *Proc. 9th Int. IAHR Symp. on Ice, 9th(1),* 152–161, 1988.

Broek, D., *Elementary Engineering Fracture Mechanics,* 4th rev. ed., Martinus Nijhoff, Boston, MA, 1986.

Butiagin, I.P., *Strength of Ice and Ice Cover* (in Russian), 154 pp., Nauka, Sibirskoe Otdelenie, Novosibirsk, Russia, 1966.

Butkovitch, T.R., Linear thermal expansion of ice, *Res. Rep. 40,* U.S. Army Cold Reg. Res. and Eng. Lab., Hanover, NH, 1957.

Curtin, T.B. (ed.), *Sea Ice Mechanics Workshop,* Office of Naval Research, Washington, D.C., 1991.

DeFranco, S.J., and J.P. Dempsey, Crack growth stability in S2 ice, *Proc. Int. IAHR Symp. on Ice, 10th(1),* 168–181, 1990.

DeFranco, S.J., and J.P. Dempsey, Crack growth stability in saline ice, in *Mechanics of Creep Brittle Materials, vol. 2,* Leicester, England, in press, 1991.

Dempsey, J.P., The fracture toughness of ice, in *Ice/Structure Interaction* edited by S. Jones et al., pp. 109–145, Springer-Verlag, New York, 1989.

Dempsey, J.P., Notch sensitivity of ice, in *Proceedings First Material Engineering Congress,* vol. 2, pp. 1124–1133, ASCE, New York, 1990.

Dempsey, J.P., Y. Wei, S.J. DeFranco, R. Ruben, and R. Frachetti, Fracture toughness of S2 columnar freshwater ice: Crack length and specimen size effects, 1, *Proc. Int. Conf. Offshore Mech. Arctic Eng, 8th(IV),* 83–89, 1989a.

Dempsey, J.P., Y. Wei, S.J. DeFranco, R. Ruben, and R. Frachetti, Fracture toughness of S2 columnar freshwater ice: Crack length and specimen size effects, 2, *Proc. Int. Conf. Offshore Mech. Arctic Eng., 8th(IV),* 199–207, 1989b.

Dempsey, J.P., Y. Wei, and S.J. DeFranco, Notch Acuity Effects on the CTOD and K_Q of Ice, in *Micromechanics of Failure of Quasi-Brittle Materials*, edited by S.P. Shah, S.E. Swartz, and M.L. Wang, pp. 333-342, Elsevier, New York, 1990.

Dempsey, J.P., Y. Wei, and S.J. DeFranco, Fracture resistance of cracking in ice: Initiation and growth, in *Cold Regions Engineering, 1991*, edited by D.S. Sodhi, pp. 579-594, 1991.

Evans, R.J., Cracks in perennial sea ice due to thermally induced stresses, *J. Geophys. Res.*, 76(33), 8153-8155, 1971.

Evans, R.J., and N. Untersteiner, Thermal cracks in floating sea ice sheets, *J. Geophys. Res.*, 76(3), 694-703, 1971.

Farmer, D.M., and Y.-B. Xie, The sound generated by propagating crack in sea ice, *J. Acoust. Soc. Am.*, 85(4), 1989, 1489-1500.

Gold, L.W., Crack formation in ice plates by thermal shock, *Can. J. Phys.*, 41, 1712-1728, 1971.

Hetényi, M., *Beams on Elastic Foundation*, University of Michigan Press, Ann Arbor, 1946.

Johnson, J.B., G.F.N. Cox, and W.B. Tucker, III, Kadluk ice stress measurement program, *Proc., Int. Conf. on Port and Ocean Eng. Under Arctic Cond.*, 8th(1), pp. 88-100, 1985.

Ketcham, W.M., and P.V. Hobbs, An experimental determination of the surface energies of ice, *Philos. Mag.*, 19, 1161-1173, 1969.

Lewis, J.K., and W.W. Denner, Higher frequency ambient noise in the Arctic Ocean", *J. Acoust. Soc. Am.*, 84(4), 1444-1455, 1988.

Milne, A.R., Thermal tension cracking in sea ice: A source of underice noise, *J. Geophys. Res.*, 77(12), 2177-2192, 1972.

Palmer, A.C., D.J. Goodman, M.F. Ashby, A.G. Evans, J.W. Hutchinson, and A.R.S. Ponter, Fracture and its role in determining ice forces on offshore structures, *Ann. Glaciol.*, 4, 216-221, 1983.

Parmerter, R.R., On the fracture of ice sheets with part-through cracks, *AIDJEX Bull.* 30, pp.94-118, Univ. of Wash., Seattle, 1975.

Parsons, B.L., The size effect of nominal ice failure pressure, fractals, self similarity and nonstationarity, *Proc. Int. Conf. on Port and Ocean Eng. under Arctic Cond. 11th* in press, 1991.

Parsons, B.L., J.B. Snellen, and B. Hill, Preliminary measurements of terminal crack velocity in ice, *Cold Reg. Scie. and Technol.*, 13, 233-238, 1987.

Parsons, B.L., J.B. Snellen, and D.B. Muggeridge, The initiation and arrest stress intensity factors of first year sea ice, *Proc. Int. IAHR Symp. on Ice*, 9th(1), 502-512, 1988.

Parsons, B.L., J.B. Snellen, and D.B. Muggeridge, The double torsion test applied to fine grained freshwater columnar ice,

and sea ice, in *The Mechanics of Creep Brittle Materials, Eur. Mech. Colloq. 239* edited by A.C.F. Cocks and A.R.S. Ponter, Elsevier, New York, 1989.

RILEM Committee TC89-FMT, Size effect method for determining fracture energy and process zone of concrete (International RILEM recommendation of standardized test), *Mater. Struct.* 23, 461-465, 1990.

Sanderson, T.J.O., *Ice Mechanics: Risks to Offshore Structures*, Graham and Trotman, Boston, MA, 1988.

Schapery, R.A., Models for the deformation behavior of viscoelastic media with distributed damage and their applicability to ice, in *Ice/Structure Interaction*, edited by S. Jones et al., New York, Springer-Verlag, pp. 229-230, 1989.

Stehn, L., Fracture toughness of sea ice, Licentiate thesis, Div. of Struct. Eng., Lulea Univ. of Technol., Lulea, Sweden, 1990.

Timco, G.W., Laboratory observations of macroscopic failure modes in freshwater ice, in *Cold Regions Engineering*, edited by D.S. Sodhi, pp. 605-614, Am. Soc. of Civil Engrs., New York, 1991.

Timco, G.W., and N.K. Sinha, Experimental results of the buckling of freshwater ice sheets, *Proc. Offshore Mech. and Arctic Eng. Symp.*, 7th(4), 31-38, 1988.

Tucker, W.B., III, and D.K. Perovich, Stress measurements in drifting pack ice, *Cold Reg. Sci. Technol.*, in press, 1991.

Urabe, N., and A. Yoshitake, Strain-rate dependent fracture toughness (K_{Ic}) of pure ice and sea ice, *Proc. IAHR 81*, vol. 2, 410-420, 1981.

Weeks, W., and A. Assur, The mechanical properties of sea ice, *Rep. II-C3, U.S. Army Cold Reg. Res. and Eng. Lab.*, Hanover, N.H., 1967.

Weeks, W., and A. Assur, A., Fracture of lake and sea ice, *Res. Rep. 269, U.S. Army Cold Reg. Res. and Eng. Lab.*, Hanover, N.H., 1969.

Weeks, W.F., and M. Mellor, Mechanical properties of ice in the Arctic seas, in *Arctic Technology and Policy*, edited by I. Dyer and C. Chryssostomidis, Hemisphere, Washington, D.C., pp. 235-259, 1984.

Z.P. Bažant, Department of Civil Engineering, Northwestern University, Evanston, Illinois 60208-3109.